THE FINE STRUCTURE OF THE URINARY BLADDER OF THE TOAD, *BUFO MARINUS*

JAE KWON CHOI, M.D.

From the Department of Anatomy, University of Washington, Seattle, and Chonnam University Medical School, Kwangju, Korea

ABSTRACT

The urinary bladder of the toad (*Bufo marinus*) was studied with both the light and the electron microscope. The bladder wall consists of epithelium, submucosa, and serosa. In the epithelium, four different cell types were recognized on the basis of their fine structure and staining properties with several different dyes. These four were designated as granular cells, mitochondria-rich cells, mucous cells, and basal cells. In addition, migratory cells of a different type were found in the basal region of the epithelium. The luminal surface of the epithelial cells presents irregular microvilli and is coated by PAS-positive material which has been further investigated by histochemical procedures and radioautography. Included is a description of the fine structural details of cell membranes, cell junctions, and intracellular components. The submucosa consists of a delicate stroma of fibroblasts and collagen fibers and also contains blood and lymph vessels, unmyelinated nerves, migratory cells, and smooth muscle cells. The serosa consists of a single layer of serosal (mesothelial) cells which form an uninterrupted covering of the viscus. Possible pathways of sodium and water transport across the bladder wall are discussed.

INTRODUCTION

In mammals, water is conserved and the salts excreted, while in amphibia the reverse is true to a large degree. Furthermore, with the less efficient regulatory mechanism of the amphibian kidney, the bladder functions not merely as a receptacle for urine, but also as a reserve supply of water under certain circumstances (45).

The toad bladder has been studied by physiological methods as a membrane which transports water, sodium, and other substances under various conditions (4, 5, 11, 15, 21–23). Not only is it a convenient organ in which to investigate certain aspects of absorption, but its relatively simple structure is well suited for morphological correlations. The toad bladder should be a model system for correlating structure and function in a living animal membrane, although there has been little attempt to do so. There exist several classical histological papers on the toad bladder (20, 25, 41) and several recent short reports (8, 9) on the fine structure. Pak Poy and Bentley (31) were the first to study changes of the fine structure of the toad bladder epithelial cells when the cells were under the influence of Pituitrin. A recent excellent paper by Peachey and Rasmussen (34) describes the fine structure of the toad bladder epithelium in considerable detail and relates the structure to water transport in different physiological states. The observations reported here are in general agreement with this latter paper, although there are some differences in detail and interpretation. The present study includes extensive observations on the fine structure of the toad bladder and attempts to provide a firm morphological basis for further experimental studies.

MATERIALS AND METHODS

Eight toads, *Bufo marinus*, were used in the course of this study. They were kept in laboratory terraria at room temperature (22°C) and fed liver by hand twice a month. They appeared to be in good health.

Bladders were fixed *in situ* by both injecting into the lumen of the bladder, and applying to its external surface, ice cold fixative (2 per cent OsO_4 in 0.1 N *s*-collidine buffer, pH 7.5 (2)). Portions of the ventral wall of the bladder about 1 cm from the midline were removed, cut into bits, and placed for 2 hours in fresh fixative cooled in cracked ice. Also, portions of bladder were fixed in permanganate (26). The specimens were dehydrated in ethanol, embedded in Epon or Araldite epoxy resins (27), and cut on a Porter-Blum microtome. Sections were stained with half-saturated uranyl acetate aqueous solution for 2 to 4 hours (46), or with lead acetate (12) or Millonig's lead stain (28), and examined in an RCA EMU-2C electron microscope. All micrographs were taken on Kodak fine grain positive film (47).

For light microscopy, tissues were fixed in OsO_4 and embedded in methacrylate. Sections were cut 1.5 μ thick with a Porter-Blum microtome using glass knives. The methacrylate was dissolved in xylene and the tissues were stained by the PAS method followed by staining in slightly alkaline 1 per cent toluidine blue in 50 per cent ethanol solution. With this stain combination, cytological preservation was good and four types of epithelial cells were differentiated easily in the sections. Slides were treated with saliva before the PAS reaction as a test for glycogen localization. Cellular identification was confirmed on thin paraffin sections cut with a Porter-Blum microtome using glass knives after fixation with Zenker-formol, neutral formol, Carnoy's fluid, or alcoholic lead nitrate (24). Further characterization of the material stained in the PAS procedure was attempted by bromination and acetylation of sections (24). Hale's colloidal iron procedures (29) were also employed.

In an attempt to label the mucous cells, four toads were injected intravenously with 140 microcuries of $Na_2S^{35}O_4$ (1 μc/gm). Tissues were fixed in Bouin's fluid at 1, 4, 24, and 48 hours after injection. The radioautography was carried out according to the procedure of Bélanger and Leblond as modified by Everett *et al.* (14) using NTB-3 liquid emulsion and 3 weeks exposure.

A. LIGHT MICROSCOPY

1. *Epithelium*

When the bladder wall is contracted, the epithelium is one or two cell layers thick, displaying cuboidal or columnar cells. In the distended condition, however, it becomes flattened and squamous. The epithelium rests on a thin basement membrane (arrows, Figs. 1 and 2). Regardless of the degree of contraction, after osmium tetroxide fixation and PAS–toluidine blue staining, it is possible to distinguish four types of cells constituting the epithelium. These are: the granular cell, the mitochondria-rich cell, the mucous cell, and the basal cell.

Most numerous of all four types is the *granular cell* (*GR*, Figs. 1 and 2), which covers most of the bladder surface. It is distinguished by a layer of PAS–positive small granules (*g*, Fig. 2) just beneath the luminal surface of the cell. These granules are poorly preserved in formalin-fixed paraffin sections, but are distinct after osmium tetroxide fixation and methacrylate embedding. Although PAS–positive, they resist saliva digestion and are basophilic, but do not stain metachromatically with toluidine blue, regardless of the fixatives used, including alcoholic lead nitrate. The PAS reaction is not prevented by bromination; however, the PAS reaction is blocked by acetylation. After acetylation, treatment with alcoholic ammonia solution fully restores the PAS reaction. These granules are darkened somewhat after osmium tetroxide fixation. There is also a distinct PAS reaction at the luminal surface of the cell. This surface layer is also positive to the Hale reaction (Fig. 4), unlike the PAS–positive granules, which do not stain with Hale's reagent. No metachromasia was detected in this layer.

The second most numerous cell is the *mitochondria-rich cell*, which occurs with a frequency of about one in eight cells in the epithelium (*MR*, Fig. 2). It is usually flask-shaped and extends through the thickness of the epithelium. The constricted neck of the flask opens to the bladder lumen, while the body of the flask lies within the epithelium and contains large numbers of mitochondria. These mitochondria show no obvious orientation or polarity of distribution in thin sections; in thick sections, the mitochondria are often packed into a dense mass which obscures cellular detail. This cell has few or no PAS–positive granules of the type which occur in the granular cell, although there is a strong PAS reaction at the apex of the cell in the form of striae (*ST*, Fig. 2) oriented normal to the epithelial surface. These mitochondria-rich cells are probably identical

with the protoplasmic cells described by Schiefferdecker (41).

The third cell type is the *mucous cell* (*MU*, Figs. 1 and 2), which occurs with the same frequency as the mitochondria-rich cells. This cell has large mucous granules concentrated in the main cell body above the nucleus, although there is some variation in the distribution of granules from one mucous cell to the next. The mucous granules are PAS–positive (*MU*, Figs. 1 and 2) and stain metachromatically with toluidine blue after osmium tetroxide fixation. The Hale reaction is also positive (Fig. 4). $S^{35}O_4$ incorporation into mucous cells was uncertain up to 4 hours. However, 24 hours after $Na_2S^{35}O_4$ injection, radioautographs showed many silver grains over the mucus in these cells (Fig. 3). There were also a few grains of silver over the epithelial surface adjacent to the mucous cell.

The fourth cell type, the *basal cell* (*BA*, Figs. 1 and 2), is small, with basophilic cytoplasm, and is located near the basement membrane. These cells have no distinct granular characteristic, but have small, deeply staining, and often indented nuclei. They are interpreted as young, undifferentiated epithelial cells.

2. *Submucosa*

Beneath the basement membrane of the epithelium is a submucosa of highly variable thickness. It is composed of a loose, interlacing feltwork of collagen bundles embedded in a matrix which contains many capillaries and venules, wandering cells, nerve fibers, and thick, distinct smooth muscle bundles. Several of these components are seen in Fig. 1. The morphology presented here is drastically altered when the bladder is distended. The smooth muscle cells reveal a PAS reaction in the perinuclear region. This reaction is prevented by prior incubation with saliva, providing evidence for identification as glycogen.

3. *Serosa*

The serosa (*SE*, Fig. 1) consists of a thin, but complete, layer of simple squamous epithelium. The serosal cells have polymorphic nuclei which bulge into the peritoneal cavity. In some regions the attenuated cytoplasm is partially obscured by adjacent collagen bundles. There is no other evidence of specialization. Characteristic granules are not found in serosal cells.

B. ELECTRON MICROSCOPY

The various cell types described above were identified in electron micrographs and the microscopic features were verified. In addition, certain other details became apparent, particularly in the case of the epithelium.

1. *Epithelium*

Although microvilli are just visible in the light microscope, it is clearly apparent in the electron micrographs that the entire luminal surface of the epithelium is populated with short microvilli (Fig. 5). Likewise, it is easily seen that the epithelium is limited from the underlying submucosa by a thin, but complete, basement membrane (*BM*, Figs. 5, 8, and 9) which follows the convolutions at the base of the epithelial cells and which is occasionally interlaced with single collagen fibrils from the submucosa (*BM*, Fig. 20). The four cell types present differences which warrant individual treatment.

The *granular cell* has dense granules about 0.3 μ in diameter (*g*, Figs. 5, 8, 12, and 18) situated in a distinct layer within several micra beneath the luminal surface. They reveal a suggestion of an internal filamentous structure (*g*, Fig. 12) under high magnification and show occasionally an external limiting membrane with the "unit membrane" structure (39) (arrows, Fig. 12). In some instances, this membrane appears to be continuous with the plasma membrane of the cell. Thus the contents of the granule may on occasion have access to the bladder lumen. The microvilli (Figs. 5, 8, and 13) are rather short (0.5 μ) and spaced about a micron apart. The length and separation vary according to the degree of stretch of the epithelium. In the dilated bladder, the microvilli are shorter and farther apart than in the contracted state. The microvilli (*MI*, Fig. 13) reveal an irregular, faint granular or fibrous internal structure which appears confluent with a filamentous zone deep to the cell surface. The cell membrane delimiting the microvilli likewise shows the "unit membrane" structure (Figs. 11 and 12), which measures about 45 to 50 A peak-to-peak distance. Extending into the bladder lumen from the outer surface of the microvillus is a pile or nap of fine filaments (Fig. 13). These appear to be finer than tonofilaments, perhaps 20 or 30 A in diameter, and about 0.5 μ in length. Their disposition with respect to the unit membrane of the microvillus is not clear. They appear

to be equivalent to the "antennulae microvillares" which Yamada (48) described in the gallbladder epithelium. These extracellular fine filaments may correspond to the PAS–positive material in light microscopy. The origin of these filaments has been assumed to be from dense granules near the luminal surface of the toad bladder epithelium (34). Possible origin and function of these filaments will be discussed later in this paper.

The lateral surfaces of the epithelial cells inter-

Explanation of Figures

Figs. 1 to 4 are light micrographs of toad bladder wall fixed in osmium tetroxide, Bouin, or Carnoy and embedded in methacrylate or paraffin. Subsequent figures are electron micrographs of toad bladder fixed in osmium tetroxide and embedded in epoxy resins.

FIGURE 1

Survey picture of the full thickness of contracted toad bladder wall, taken from osmium tetroxide–fixed, methacrylate-embedded tissue. Slide was stained by the PAS method followed by toluidine blue. Above is the epithelium, showing several cell types. Granular cells (*GR*) with superficially located PAS-positive granules (black), basophilic cytoplasm, and round or oval nuclei are the most numerous. Three mucous cells (*MU*) and several basal cells (*BA*) with small, densely stained nuclei can be seen also. Mitochondria-rich cells cannot be identified in this picture. Below is the serosa (*SE*), characterized by cells with polymorphic nuclei bulging into the coelom and with pale and attenuated cytoplasm. In some regions, the attenuated cytoplasm is obscured by adjacent collagenous fiber bundles. The submucosa varies in thickness. Thicker portions contain several blood vessels (*BV*) lined by attenuated endothelial cells, smooth muscle bundles (*SM*), and unidentified cellular elements immersed among the collagenous fibers running in various directions. In the thin regions, few cells and lesser amounts of collagenous fibers are evident. Arrows indicate basement membrane. × 800.

FIGURE 2

Section was prepared the same way as Fig. 1 (oil immersion); lumen at the top. The irregularly contoured luminal surface is coated with PAS-positive material. The PAS-positive basement membrane (arrows) is seen between epithelium and submucosa. Four different cell types are easily discernible: granular cells (*GR*) with PAS-positive granules (*g*, black); mitochondria-rich cells (*MR*) with mitochondria (diffuse gray) and few PAS granules in the cell body; mucous cells (*MU*) showing different amounts and positions of PAS-positive globules; and basal cells (*BA*) with lobulated nuclei. Note the apical region of the mitochondria-rich cell. Its filamentous network (*ST*, PAS-positive) is continuous with the general luminal surface. Both are coated heavily by PAS-positive material. × 2900.

FIGURE 3

A radioautograph showing several granular cells and one mucous cell 48 hours after $S^{35}O_4$ administration into blood vessel. Note distribution of silver grains; they are abundant in the mucous cell and along the luminal surface of the epithelial cells, especially near the mucous cell, but there are few grains in the cytoplasm of the epithelial cells. Fixed in Bouin, stained with hematoxylin and eosin. × 1000.

FIGURE 4

A light micrograph comparable in magnification to Fig. 1, showing the Hale reaction in the contracted bladder wall. Positive staining is seen specifically at the luminal surface and in the mucous cell (*MU*). A faint indication of the basement membrane may be seen at the point of the arrow. The tissue was fixed in Carnoy, embedded in methacrylate. Thin sections (2 μ) stained with Mowry's modification of the Hale reaction. × 800.

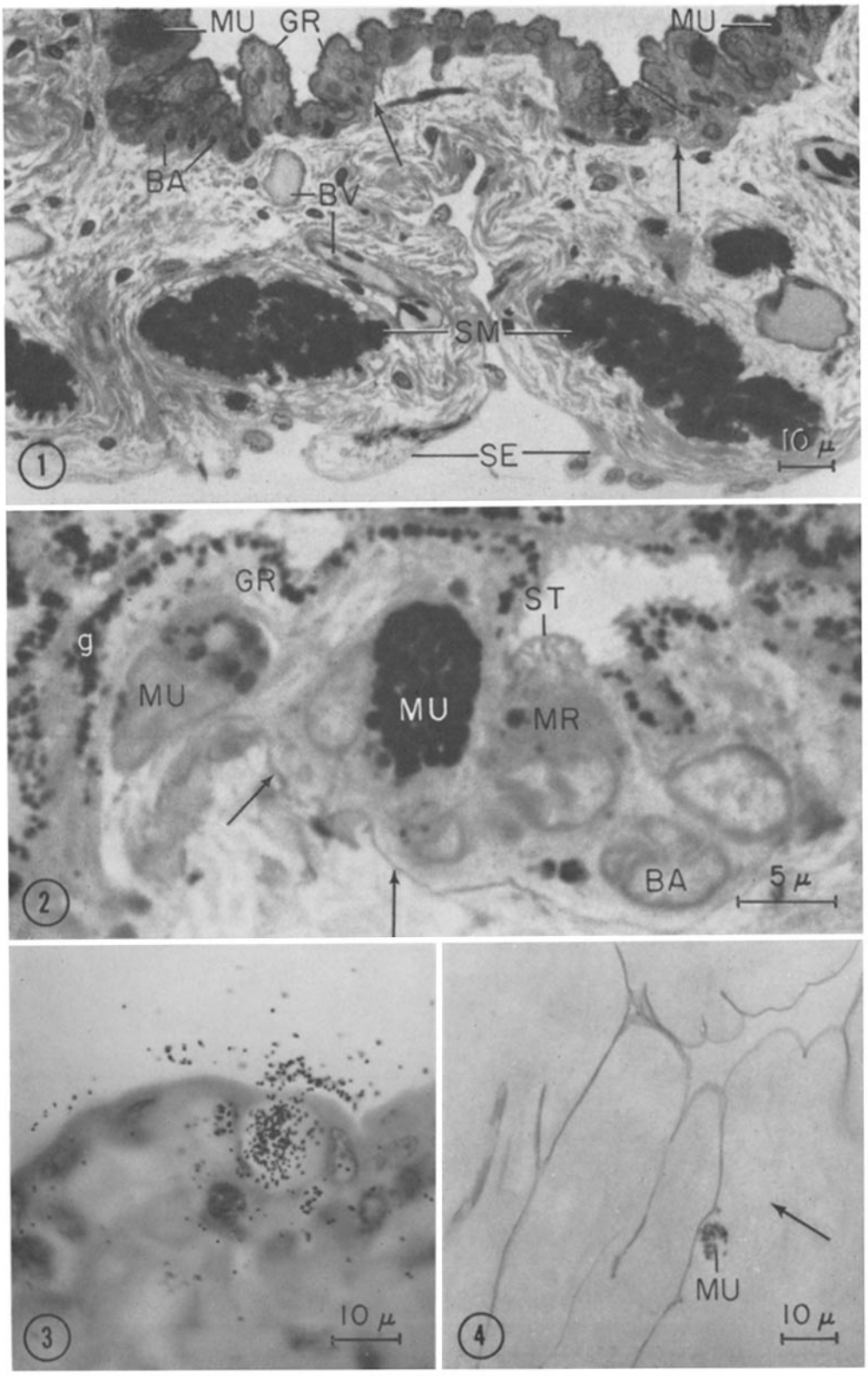
MU
GR
MU
BA
BV
SM
SE
10 μ
1
GR
ST
g
MU
MU
MR
BA
5 μ
2
10 μ
3
MU
10 μ
4

digitate with those of adjoining cells to form tortuous boundaries across the epithelium (*I*, Figs. 8 and 18). A terminal bar with typical desmosome structure (*TB*, Figs. 8, 10, and 18) is found regularly between opposing cell surfaces close to the lumen. Tonofilaments converge from the cytoplasm upon the desmosome (*DE*, Fig. 18). Commonly seen on the luminal side of the terminal bar is a specialization of the two adjacent cell membranes. In this region, the space between the two unit membranes of the adjoining cells is obliterated and the external dense components of the two unit membranes fuse to give a central dense line (arrow 1, Fig. 10; arrow, Fig. 11). Where there previously existed four dense lines (two from each unit membrane), a narrow dense triplet appears. In pictures at lower magnification the central line is not always resolved; therefore, the structure appears as two dense lines with a region of intermediate density (about 100 A in width) between the two lines. Although lateral cell surfaces are usually in close contact with adjacent cells, the basal surfaces of the epithelial cells frequently show irregular extracellular spaces (*IS*, Fig. 9) into which cytoplasmic folds may project, giving the appearance of microvilli.

The granular cells possess a Golgi complex (*G*, Fig. 8), similar to that found in other epithelia, located lateral to, or above, the nucleus. Mitochondria are frequent but not remarkable. Rough- and smooth-surfaced endoplasmic reticulum is occasionally found in the cytoplasm, more commonly at the lateral or supranuclear level. Vesicles are abundant near or along the lateral or basal membranes of the cell, but are sparse at the luminal surface. One or two typical multivesicular bodies (44) are also found in the supranuclear region. After Millonig's lead stain, glycogen is found throughout the cytoplasm as dense irregular granules (arrow, Fig. 18). Glycogen particles exhibit a fine particulate structure as described by Revel *et al.* (36). These subunits consist of dense dots approximately 35 A in diameter (Fig. 17).

The *mitochondria-rich cell* is illustrated in Figs. 5, 6, 9, 14, and 15 (*MR*). These cells have a variable abundance of mitochondria in their cytoplasm which distinguishes them from the other residents of the epithelium. The mitochondria occur predominantly in the body of the flask distributed around the nucleus. They vary in size and number from one mitochondria-rich cell to another, and, although the mitochondria may be the same size

FIGURE 5

A low magnification electron micrograph of the full thickness of the epithelium at the folded portion of the toad bladder. The lumen (*L*) is at the top and down the center. At the right lower corner is the basement membrane (*BM*) and a portion of submucosa. The epithelium reveals two layers of three different cell types: granular cells (*GR*) with dense round or oval granules (*g*); mitochondria-rich cells (*MR*) showing flask- or sac-like shapes; and basal cells (*BA*) with indented nuclei. Luminal surfaces of the cells have irregular cytoplasmic projections; lateral cell boundaries show irregular infoldings. Araldite-embedded, uranyl acetate stain. × 4200.

FIGURE 6

A low power electron micrograph of toad bladder illustrating three different cell types. (1) mucous cell (*MU*) with dense round mucous globules in the rather dense cytoplasmic matrix; at the luminal surface are a few slender cytoplasmic projections; (2) mitochondria-rich cell (*MR*) with tubules or intermicrovillous spaces (arrows) cut longitudinally; next to this region, many dense vesicles and tubules are seen; (3) granular cells (*GR*) with dense granules. Araldite-embedded, uranyl acetate stain. × 4300.

FIGURE 7

A low power electron micrograph showing another type of mucous cell (*MU*) which has coalesced mucous material in the supranuclear region and a slender stalk from the cell body to the basement membrane (*BM*), where the stalk terminates in an arborization. Araldite-embedded, uranyl acetate stain. × 4200.

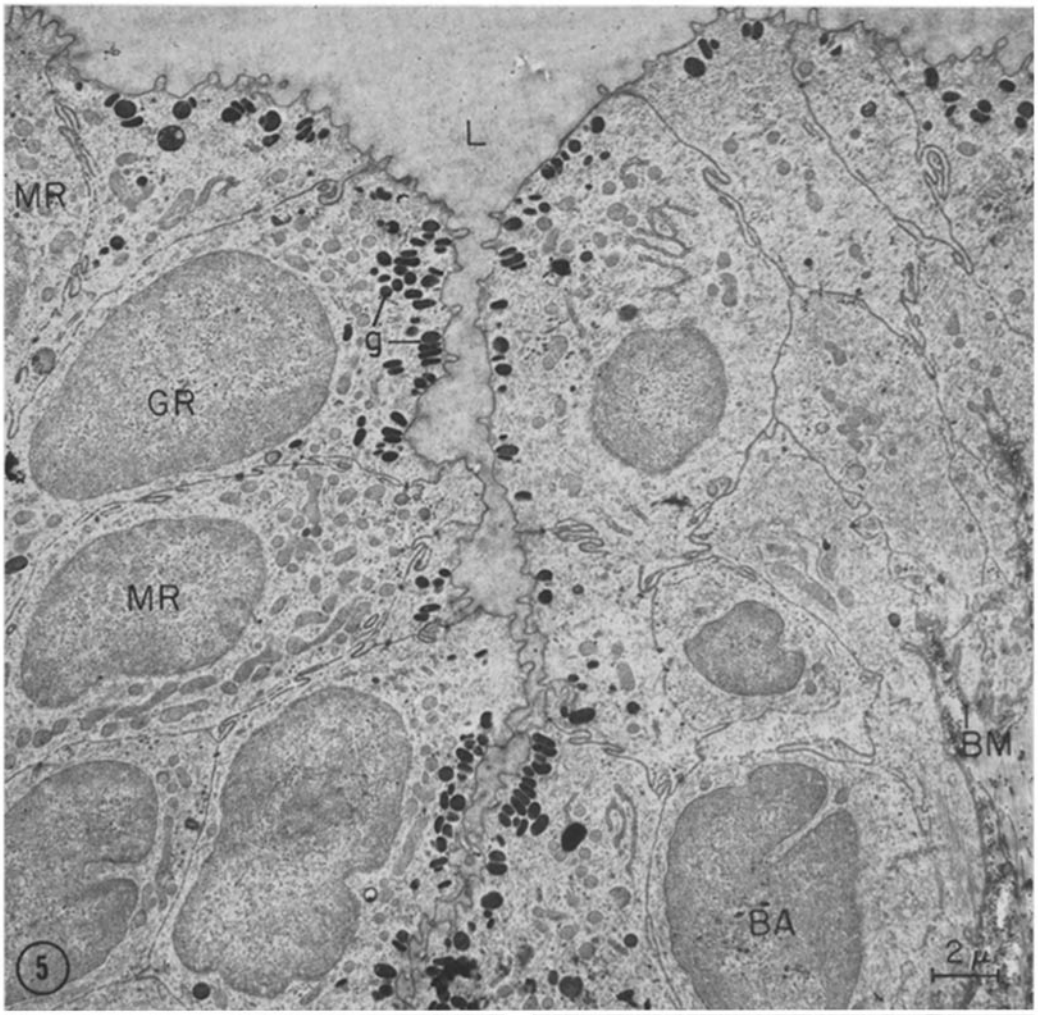
L
MR
g
GR
MR
BM
BA
2μ
5

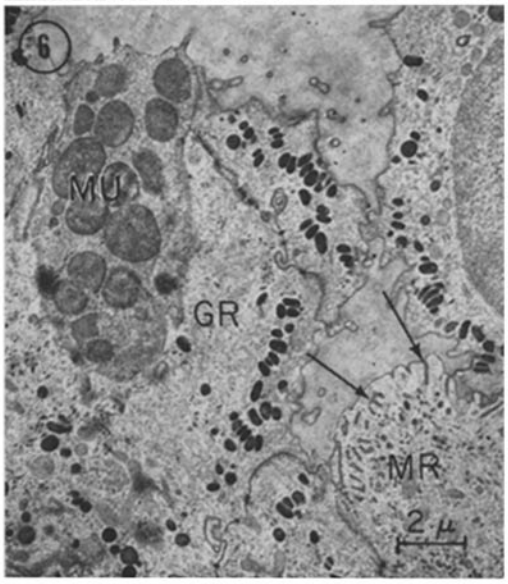
6
MU
GR
MR
2μ

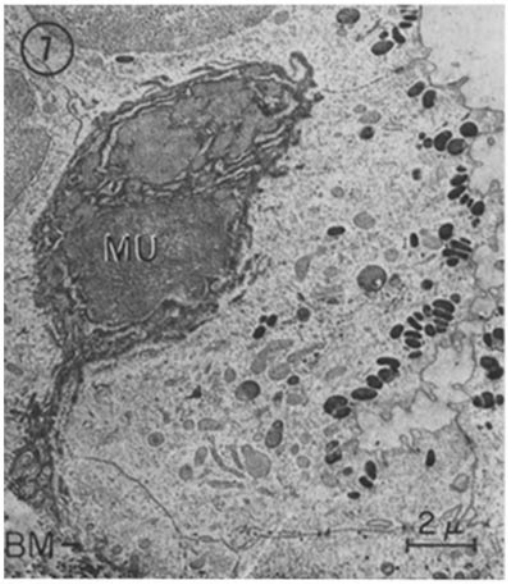
7
MU
BM
2μ

as, or larger than, those of other cells, they are never smaller. These mitochondria usually contain a few dense granules several hundred angstroms in diameter, as do many other mitochondria. The matrix often varies in density from cell to cell.

A second characteristic of this cell is the neck of the flask, which protrudes into the bladder lumen and is provided with microvilli (*MR*, Figs. 5 and 6; Fig. 14). The microvilli are highly variable in width and length in comparison with those of the granular cell. Sometimes the luminal surface membrane with its coating of extracellular substance invaginates deeply into the apical cytoplasm (*MR*, arrows, Fig. 6; Fig. 14) to give the appearance of large tubules and vesicles about 0.1 to 0.2 μ in diameter. These intervillous spaces or tubules give rise to the apical striation noted in these cells by light microscopy.

Numerous small vesicles and tubules about 500 A in diameter also are scattered throughout the cytoplasm of these cells, but are particularly concentrated in the neck region (*V*, Figs. 14 and 15). Any order in orientation of these small vesicles and tubules is not obvious. There is little membranous endoplasmic reticulum in these cells, but multivesicular bodies (*MV*, Figs. 14 and 15) have been seen often in the neck region. The Golgi apparatus in these cells is fragmented into several units. Fig. 9 (*G*) shows a portion of one such Golgi unit.

The electron microscope observations of the *mucous cell* reveal little that is new other than what has already been described for these cells (32, 38). Figs. 6 (*MU*) and 7 (*MU*) show such cells, with their content of mucin granules. After Millonig's lead stain, considerable numbers of particles presumed to be glycogen are found between the granules (Fig. 16).

The *basal cell* (*BA*, Figs. 5, 9, and 20) is normally an inconspicuous, irregularly shaped cell, but in the distended bladder it occasionally appears flattened. The cytoplasm is generally more dense than that of the granular cells. The nuclei of the basal cells often show indentations. Cellular components such as mitochondria and Golgi apparatus are found in minimum amounts, but there appears to be an increased amount of intracellular filaments (*f*, Figs. 9 and 20) as compared with the granular cells.

2. *Submucosa*

The bulk of the submucosa is made up of small collagenous bundles and single collagen fibrils (*CF*, Figs. 8 and 20) running in various directions. These fibers are embedded in a substance of low electron opacity which reveals no structure at this level of resolution. Narrow or broad condensations of material of similar appearance are seen at cell borders, separated from the cell membrane by a pale zone several hundred angstroms wide, to form basement membranes (*BM*, Figs. 5, 8, 9,

FIGURE 8

Micrograph of a slightly oblique section of the epithelium showing several granular cells. The lumen (*L*) is above and down the center. The basement membrane (*BM*) and collagenous fibers (*CF*) can be seen at the bottom corners. The luminal surface has irregular microvilli. The terminal bars with desmosome (*TB*) are also seen. Lateral cell boundaries are straight at *S*, but elaborate infoldings are present at *I*. Dense granules (*g*) aligned beneath the luminal surface are prominent. Mitochondria are distributed mainly next to the dense granules. There are a few isolated strands of ER with RNP particles. A Golgi region (*G*) with cisternae and vesicles can be seen. Araldite-embedded, uranyl acetate stain. × 8600.

FIGURE 9

An electron micrograph showing portions of a basal (*BA*) and a mitochondria-rich cell (*MR*). The basal cell (lower left) lies adjacent to the basement membrane (*BM*) and contains an indented nucleus (*N*) with a nucleolus (arrow), Golgi region (*G*), and cytoplasmic filaments (*f*); a few small mitochondria and vesicles also are seen. A process of the basal cell is seen extending to the right. The mitochondria-rich cell (upper right) also shows a Golgi region (*G*), numerous mitochondria, and several unidentified round bodies (*RB*). A wide intercellular space (*IS*) is sometimes found in the basal region of the epithelium, as demonstrated by the picture. Epon-embedded, Millonig's lead stain. × 19,000.

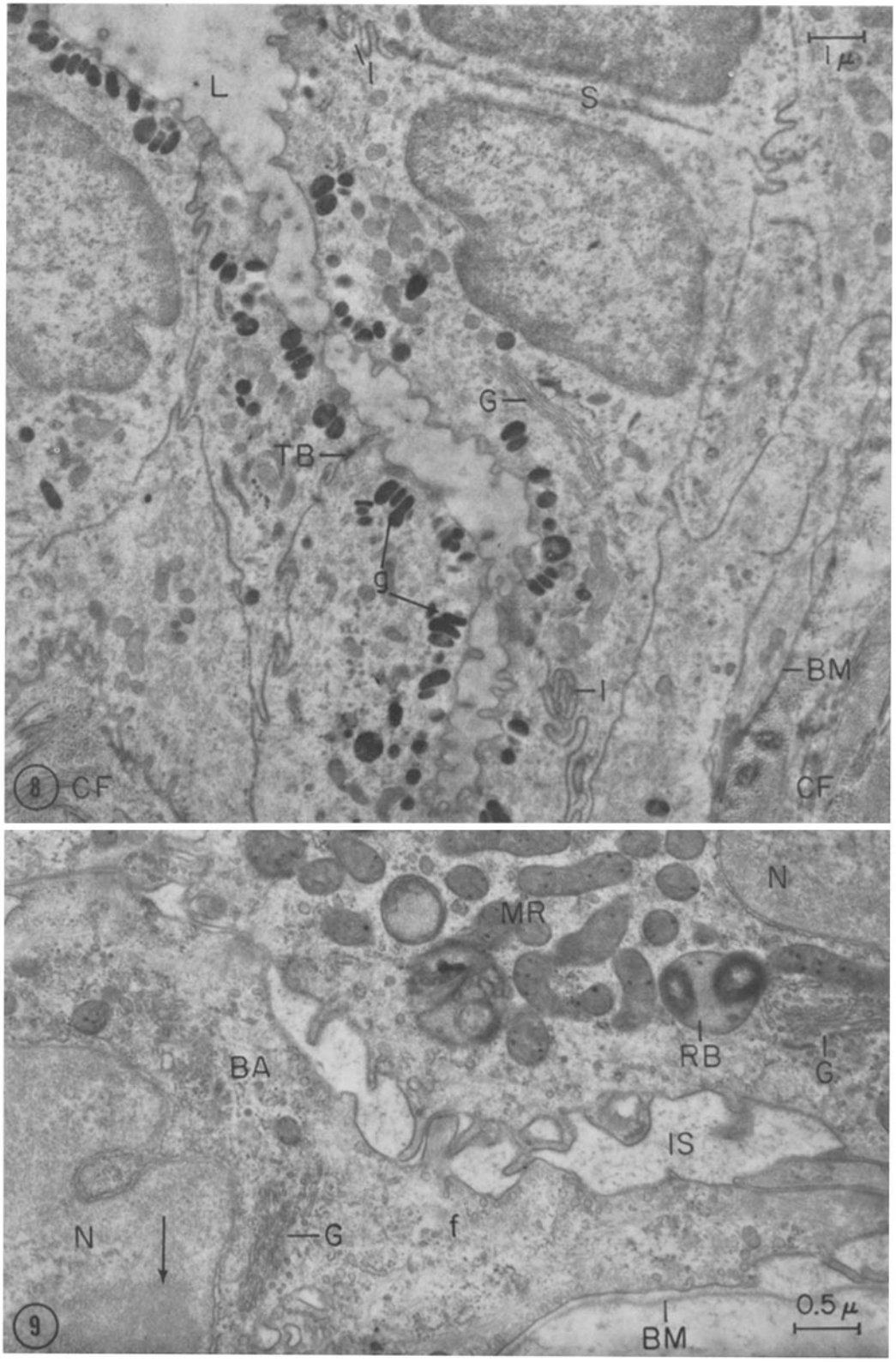
1 μ
L
I
S
G
TB
g
I
BM
8
CF
CF
N
MR
RB
G
BA
IS
N
G
f
9
BM
0.5 μ

and 20). Coursing through this loose feltwork are capillaries or venules of the A-1-α type, according to the classification of Bennett *et al.* (3). The endothelial cytoplasm forms a complete but attenuated lining with many vesicles and caveolae, but with no visible pores (*EN*, Fig. 20). Basement membranes and pericapillary cells are not remarkable. Occasional thin unmyelinated nerve fibers (*NE*, Fig. 20) are encountered, as are sheets or processes of cytoplasm (*P*, Fig. 20), presumably extended from fibroblasts or wandering cells. All the foregoing features are illustrated in Fig. 20. Also found, but not illustrated, are lymphatics, conforming to the description given by Fraley and Weiss (17), with thin endothelial walls which have little or no basement membrane and no gaps between cell junctions. The smooth muscle cells contain cytoplasmic fibrils, but the fibrils are not resolved in the accompanying figure (Fig. 19). No cytoplasmic connections to adjacent smooth muscle cells have been seen. Considerable amounts of glycogen are found in the perinuclear region after lead staining. This confirms the findings from light microscopy using the PAS reaction described above under Light Microscopy.

3. *Serosa*

In the electron micrographs the serosa is seen to be composed of a single layer of flattened cells. The cytoplasm is highly attenuated both in the

FIGURE 10

A high power electron micrograph showing the area between two adjacent cells near the lumen (*L*). At the left are low projections of the adjacent cell surfaces. The unit structure of the surface membrane is not apparent over part of the projections where obliquity and a nap of external filaments obscure the membrane. The area of cell contact nearest the lumen appears fused to form a "tight junction." In this area, the intercellular space appears to be obliterated by fusion of outer dense components of the two unit membranes, giving rise to three dense lines (arrow 1). Next to the "tight junction" is the terminal bar (*TB*) with a prominent desmosome. In the terminal bar region six continuous linear densities plus a discontinuous central density are apparent in the basal or right hand half of the structure. Two of the dense lines on each side appear to be continuous with the unit structure of the cell membrane (arrow 2). Associated with the terminal bar are intracellular filaments cut in various directions. Epon-embedded, uranyl acetate stain. × 218,000.

FIGURE 11

A high power electron micrograph showing a "tight junction" area of plasma membranes near the luminal surface between two granular cells. At the left a microvillus (*MI*) covered by unit membrane projects into the lumen (*L*). The external dense component of each of the unit membranes of the two cells appears to be fused to give a central dense line (arrow). Epon-embedded, uranyl acetate stain. × 178,000.

FIGURE 12

A high power electron micrograph showing the surface of a granular cell with a dense granule (*g*) surrounded by a membrane which shows the unit structure (arrows). The enveloping membrane appears to be continuous with that covering the surface of the cell. The luminal end (*L*) of the granule is devoid of membrane. Note the suggestion of a fine filamentous structure within the dense granules. Araldite-embedded, uranyl acetate stain. × 104,000.

FIGURE 13

A high power electron micrograph showing microvilli (*MI*) and hair-like filaments (antennulae microvillares) extending into the lumen (*L*) from the microvilli and the surface membrane. The plasma membrane covering the base of the microvillus at the left center continues for some distance. A "tight" junction area (arrow) where membranes of two adjacent cells are fused is also seen. Araldite-embedded, uranyl acetate stained. × 93,000.

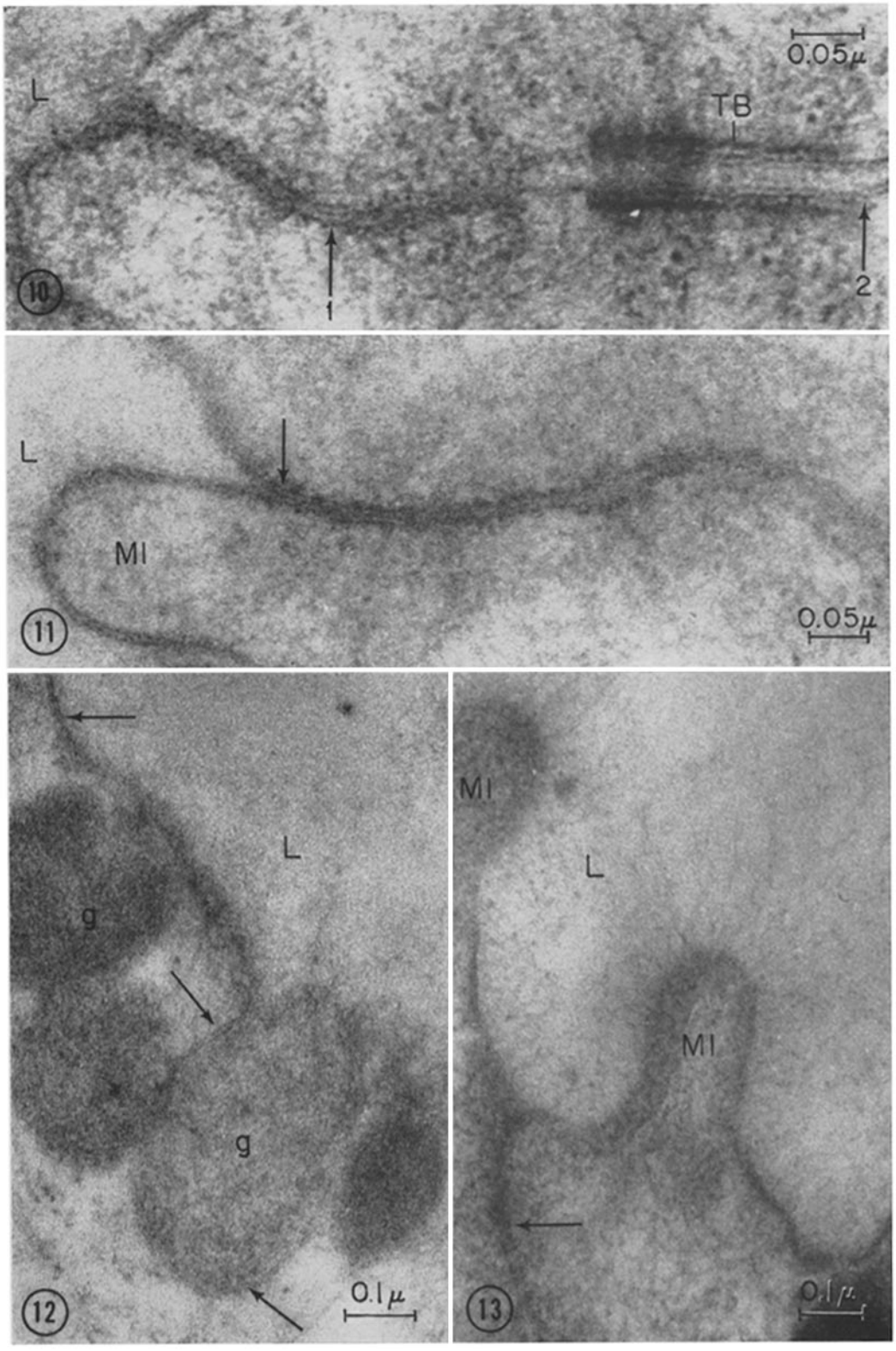
0.05μ
L
TB
1
2
10
L
MI
11
0.05μ
L
g
g
12
0.1μ
MI
L
MI
13
0.1μ

periphery of the cell and over the nucleus, which bulges into the coelom. The serosa forms a complete unperforated sheet, although previous investigators have suggested that this surface is incomplete (20, 34). Despite its thinness, many vesicles are seen in the serosal cytoplasm, with caveolae positioned at both coelomic and submucosal surfaces. Counts reveal roughly equal numbers of caveolae at both surfaces. Cells appear to be joined together at their edges by terminal bars (*TB*, Fig. 21); however, desmosomes are not found between serosal cells. Relatively few mitochondria appear in the serosal cytoplasm, and these are small and tend to aggregate near the nucleus. There is relatively little membranous endoplasmic reticulum. The serosal epithelium rests upon a thin, but distinct, basement membrane (*BM*, Fig. 21).

DISCUSSION

Many epithelia transport materials across their surfaces, including water, ions, and various nonelectrolytes (13). The transfer is called passive if it can be accounted for by ordinary physical forces such as a concentration gradient, an electrical gradient, a solvent drag, or any combination of these. It is called active if the transport cannot be explained as a result of these forces but involves participation of some energy-yielding chemical reactions (19). Instances of active transport are known to occur in a wide variety of animals and organs, and the mechanism of active transport is a fundamental problem in biology.

Physiologists have demonstrated that the toad bladder can accomplish at least passive transport of water and urea and active transport of sodium (21, 22) and that sodium transport utilizes energy derived both from glycolysis and from oxidative metabolism (5, 21, 23). These studies indicate that the transport rates rise considerably in the presence of Pitressin. The site of transport, particularly that of the active element, and the site of hormone action are not known for certain. So far, neither the mucosa nor the serosa has been

FIGURE 14

An electron micrograph showing the apical region of a mitochondria-rich cell. Irregular microvilli extend into the lumen (*L*) although in this picture the irregularity may be accentuated by oblique sectioning. Note a pile or nap of fine filaments (antennulae) extending into the bladder lumen from the surface membrane. The filaments appear to be thinner near the cell surface. The cell cytoplasm contains multivesicular bodies (*MV*), many dense vesicles (*V*), and numerous mitochondria. Epon-embedded, Millonig's lead stain. × 26,000.

FIGURE 15

An electron micrograph showing a portion of a mitochondria-rich cell fixed in potassium permanganate. The cell shows abundant distinct vesicles (*V*) and tubules packed in the apical region. Numerous mitochondria, a typical multivesicular body (*MV*), and a nucleus (*N*) with double nuclear envelope and pores (lower arrows) are seen. The granules beneath the surface membrane of granular cells do not retain their density after short potassium permanganate fixation, but their limiting membranes remain, some of which show continuity with the surface membrane (upper arrow). Epon-embedded, lead acetate stain. × 23,000.

FIGURE 16

An electron micrograph illustrating a mucous cell of the type with large mucous granules and glycogen particles. Between the mucous granules are many dense particles which are interpreted as representing glycogen. Epon-embedded, Millonig's lead stain. × 19,000.

FIGURE 17

A high magnification electron micrograph of glycogen particles seen in the cytoplasm of the granular cell. Each irregularly shaped particle shows subunits composed of electron-scattering dots approximately 35 A in diameter. Epon-embedded, Millonig's lead stain. × 220,000.

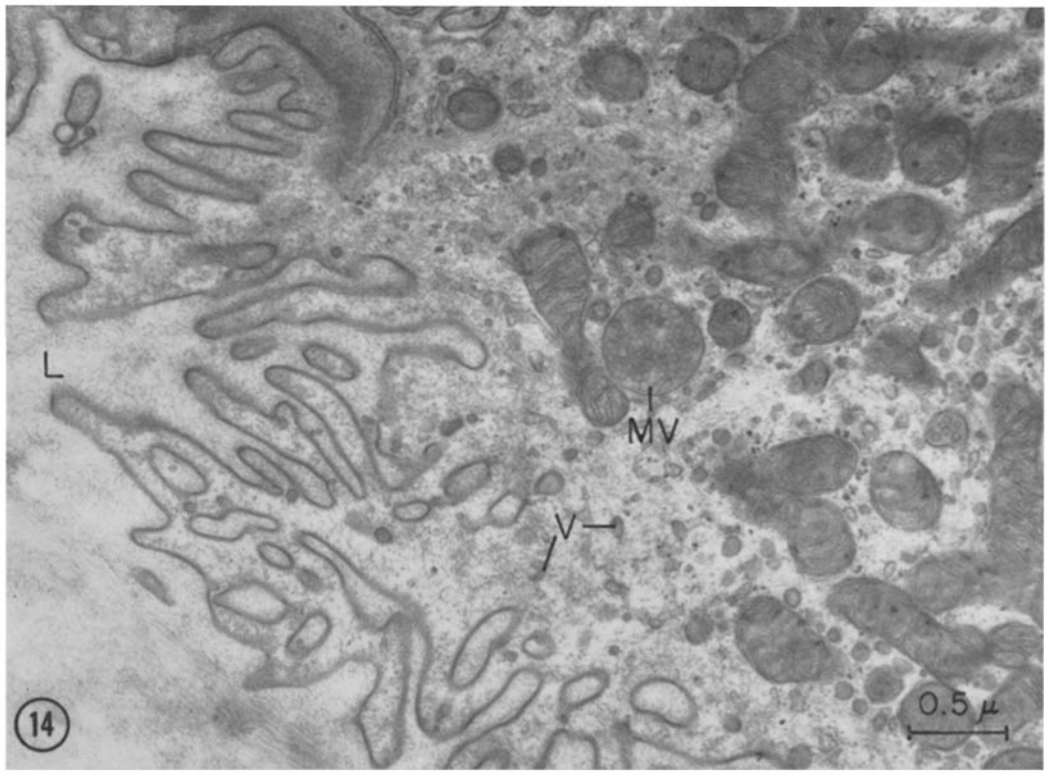
L
MV
V
0.5 μ
14

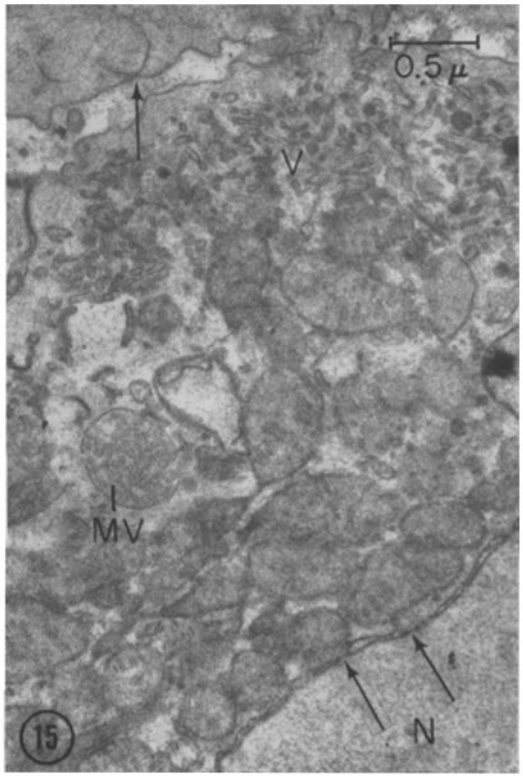
0.5 μ
V
MV
N
15

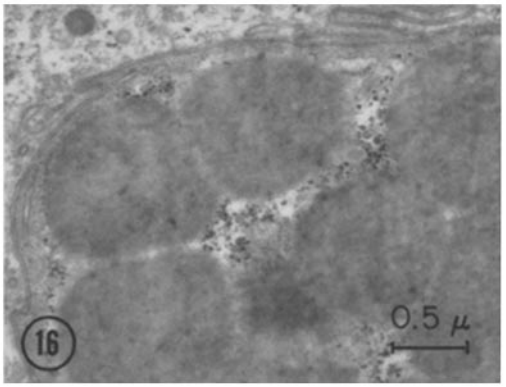
0.5 μ
16

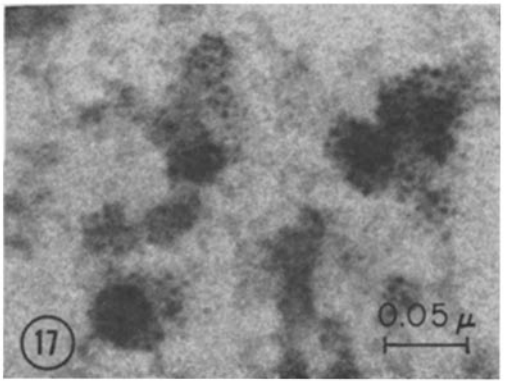
0.05 μ
17

excluded from consideration. Conventional light microscopy has not provided an answer (20, 25, 41). It may be that electron microscopy with its advantage of 100-fold improvement in resolution will do little better, but the possibility must be explored. Peachey and Rasmussen (34) have performed experiments which indicate that the site of passive water transport is the epithelial cell, but they provide no information regarding the site of active sodium transport.

Substances absorbed from the bladder may appear in the coelom and lymph spaces after injection of Pituitrin (15), or possibly appear directly in the circulation by absorption in the blood and lymph capillaries of the submucosa. Physiological experiments usually involve the study of transport across the entire bladder wall from bladder lumen to coelom, and the discussion will be directed toward this pathway. Thus, it appears that a penetrating particle moving from the bladder lumen into the coelom would have to pass the following barriers:

1. Through the epithelium, taking at least one of four possible routes:
   a. Through the granular cell
   b. Through the mitochondria-rich cell
   c. Through the mucous cell
   d. Through the intercellular space between any of the above cells
2. Through the basement membrane of the mucosa
3. Through the submucosa (by-passing any of the contained structures which are continuous in only one dimension)
4. Through the basement membrane of the serosa
5. Through the serosa, again with the possible choice of:
   a. Through the serosal (mesothelial) cell
   b. Through the intercellular space between serosal cells.

Unless the pathway of substance is between cells in mucosa or serosa (1 *d* or 5 *b*), it must pass through at least two cells in those same layers in course of penetration. There are specialized structures placed in the intercellular spaces between cells which may or may not behave as diffusion barriers. Between cells in the epithelium are terminal bars which seem to be continuous girdles about the cells, and which present a desmosome-like structure in cross-section (*TB*, Figs. 8, 10, and 18). On the luminal side of the terminal bar is a further specialization of the cell membrane taking the form of a narrowing of the intercellular space to the point that the space seems to vanish. The unit membranes which constitute the cell membranes of the adjacent cells seem to make contact, with fusion of the external layers of the unit structures to produce a new zone showing three dense lines (arrow, Figs. 10 and 11). This same pattern appears under certain conditions in the myelin sheaths of peripheral nerve (the ex-

FIGURE 18

An electron micrograph showing a slightly oblique section of granular cells with dense granules (*g*). The lumen (*L*) is at the upper left. The dense particles (arrow) not associated with membranes seen throughout the cytoplasm are probably mostly glycogen particles. Desmosomes (*DE*) are seen in the terminal bar (*TB*) and at the cell margins. Arrays of endoplasmic reticulum (*ER*) and cell infoldings (*I*) with accompanying vesicles are evident. At the lower right is an unidentified cell (*UC*) with pale cytoplasm and a large nucleus. Epon-embedded, Millonig's lead stain. × 23,000.

FIGURE 19

An electron micrograph showing portions of two smooth muscle cells cut longitudinally The nucleus (*N*) is indented. Closely packed mitochondria, multivesicular bodies (*MV*), and vacuoles with myeloid figures (*MY*) are seen in the perinuclear region. Abundant glycogen particles (small dense particles) are also present in this area. Note the cell membranes of the smooth muscle fiber. Some portions (arrow *1*) are dense with very few vesicles, but in other areas (arrows *2*) the membranes appear as fine dense lines associated with many vesicles. Two distinct types of vesicles can be seen. One group consists of many smaller vesicles of similar size limited by a thin membrane (*NE*). These are interpreted as nerve endings. The other group consists of smaller numbers of larger vesicles of mixed sizes associated with the muscle cell membrane. Epon-embedded, Millonig's lead stain. × 21,000.

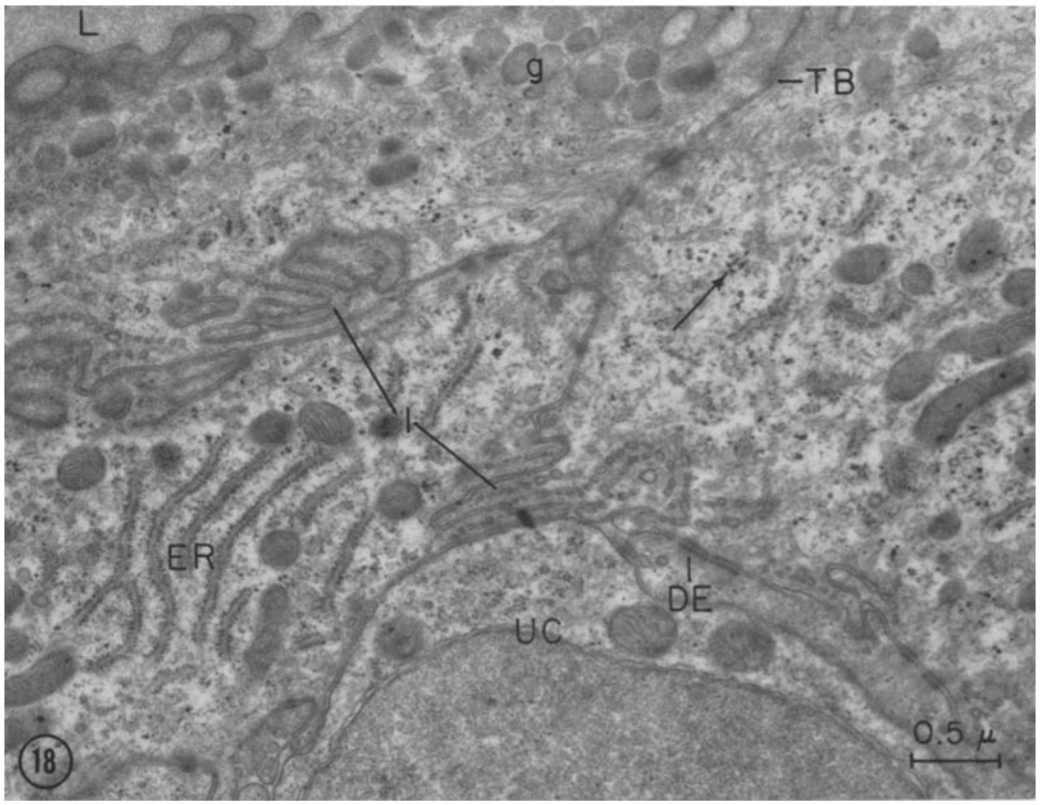
L
g
TB
I
ER
DE
UC
0.5 μ
18

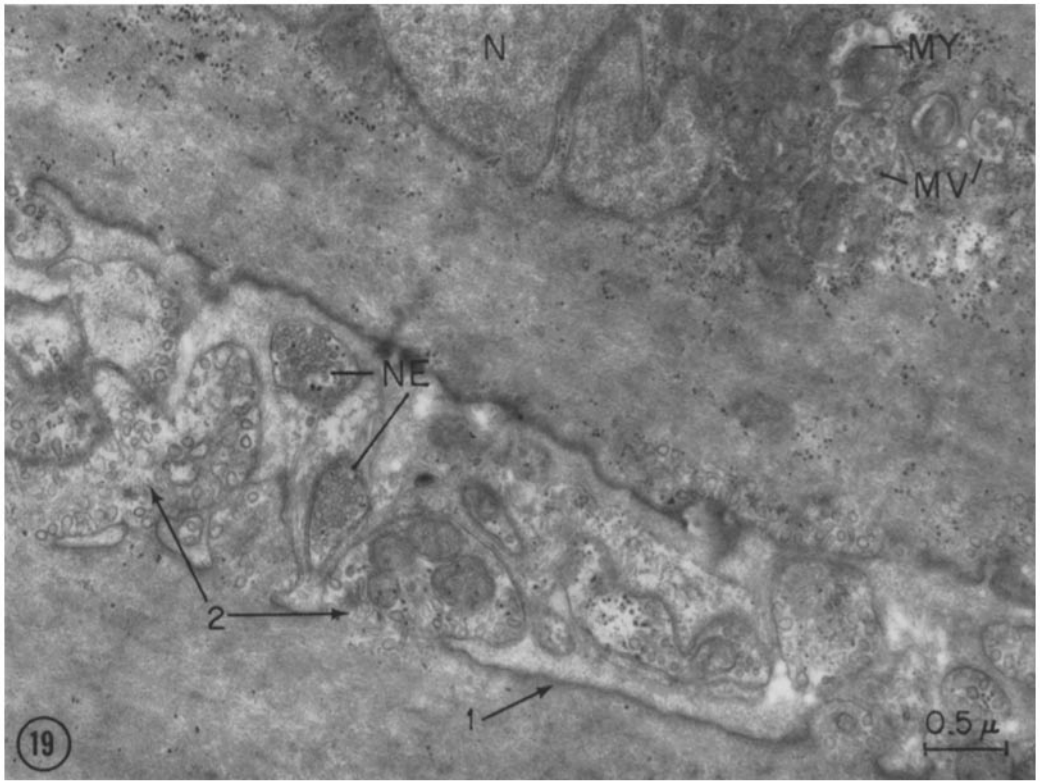
N
MY
MV
NE
2
1
0.5 μ
19

ternal compound membrane of Robertson (40)) and has recently been termed a "tight junction" by Farquhar and Palade (16). Its function as a liquid seal has been suggested by Muir and Peters (30). This may support the suggestion made previously (31, 34) that free fluid movement through the "tight junction" of the toad bladder epithelium is unlikely. After Thorotrast administration into the bladder through the cloaca, the colloidal particles are seen to be transported slowly into the cytoplasm of the epithelial cells by vesiculation, but no particles are found in the intercellular space below the "tight junction" region described above (10). Intercellular attachments (*TB*, Fig. 21) are likewise present as continuous terminal bars between serosal cells.

The two basement membranes and the ground substance of the submucosa are unlikely locations for active transport because they appear to be extracellular secretion products and presumably have no access to metabolic energy sources which are normally intracellular. Leaf *et al.* (22) and Leaf (21) have shown that 10 to 110 mv transmembrane potentials can be measured regularly across the isolated toad bladder immersed in Ringer's solution, with the serosal side positive with respect to the mucosal side. A current can be drawn from this potential source, and the current flowing can be accounted for entirely in terms of active transport of sodium ions from mucosa to serosa. Any cells within the submucosa actively involved in such electrical activity would have in parallel with themselves a large, low resistance shunt of ground substance and would seem to be improbable candidates for the seat of active transport or transmembrane potential.

If it is assumed that the transported substance moves through the cells, then some of the intracellular structures described herein may be significant. The mucous cell cannot be ruled out; Biedermann (6) suggested that the most consistent feature common to epithelia which generated a potential was the presence of mucous cells. The mechanism, however, remains obscure.

Both the granular cell and the mitochondria-rich cell are worthy of consideration as the site of transport processes. The granular cell is more frequent by far, but the mitochondria-rich cell has a large and obvious supply of oxidative energy in the form of abundant mitochondria. There is a close morphological parallel with the parietal cell of the stomach (18, 42, 43) which is quite likely the source of HCl. Both cell types have microvilli and a large complement of vesicles which have been associated previously with transport processes (33, 35, 37).

Intracellular or transcellular transport of both electrolytes and non-electrolytes by a process of vesiculation and membrane flow has been proposed by Bennett (1). Selective ionic transport by this mechanism must involve selective binding near or in the cell surface. The PAS-positive layer at the bladder surface might behave as a cationic ion exchanger to be subsequently engulfed by

FIGURE 20

An electron micrograph showing a portion of the submucosa. At the top is a portion of a basal cell (*BA*) showing nucleus (*N*), mitochondria, vesicles, and filaments (*f*). A homogeneous basement membrane (*BM*) is seen at the base of the epithelium and around the blood vessel. At the lower left is a vessel with three endothelial cells (*EN*), one with a nucleus (*N*). A few mitochondria and many vesicles are present in the endothelial cells. Note the subareas of contact (arrows)between the endothelial cells. At the lower right is an unmyelinated nerve in cross-section (*NE*). The collagen fibers (*CF*) and the elongated cell process (*P*), possibly of a fibroblast, are also seen. Epon-embedded, uranyl acetate stain. × 13,000.

FIGURE 21

Portions of two serosal cells. Elongated processes from two cells meet at *TB*, where increased density and a narrow intercellular space are interpreted as the terminal bar. Note the numerous vesicles and caveolae. Some vesicles show little internal density but have a distinct surrounding membrane which may connect to the cell membrane. There are a few small mitochondria with few cristae. Some of the dense particles scattered throughout the cytoplasm may be glycogen. The basement membrane (*BM*) is also clearly seen. Epon-embedded, Millonig's lead stain. × 26,000.


N
f
BA
BM
CF
P
EN
NE
N
1 μ
20

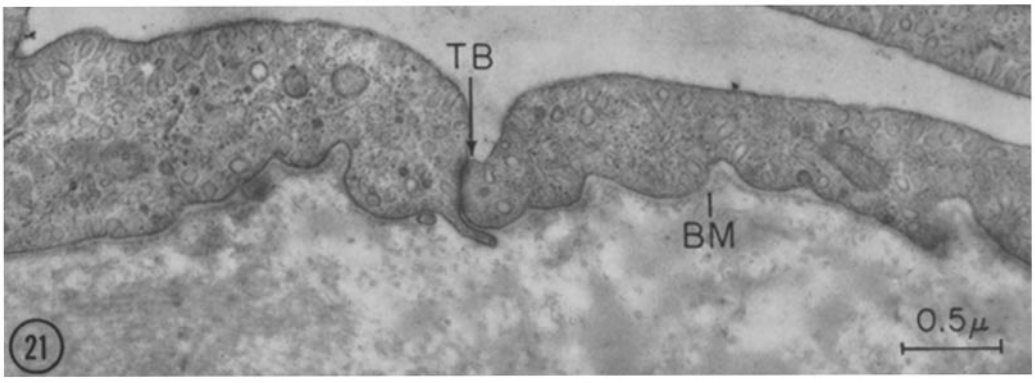
TB
BM
0.5μ
21

the cells of the epithelum. Numerous attempts were made to detect metachromasia with toluidine blue on either paraffin- or methacrylate-embedded tissue. Although the mucous granules of the mucous cells were strongly metachromatic in both circumstances, no metachromasia was detected in the PAS-positive layer. This negative result would suggest that the PAS-positive materials in the mucous cells and on the cell surface may not be identical, or that the test for metachromasia in the surface layer is too insensitive. However, the positive Hale reaction on the PAS-positive layer and in mucous cells alike suggests a close similarity. The $S^{35}O_4$ labeling experiment indicating sulfate incorporation shows localization over the mucous cell and some faint localization over the luminal surface of the epithelium, but this latter localization is poor and close to background level. Such sulfated polymers might be active cationic exchange resins. Coatings of such polymers have been described as an amorphous layer rich in mucopolysaccharides on the cell membrane of active absorbing cells (7). However, contributing to the evidence against vesicular transport in this epithelium is the observation by Pak Poy and Bentley (31) and Peachey and Rasmussen (34) that Pitressin, which accelerates both water and sodium transfer, does not appreciably alter the number of vesicles or infoldings.

The dense PAS-positive granules which are found in the granular cells within several microns beneath the luminal surface are unexplained. Histochemical study indicates that these granules contain carbohydrates; the slight blackening observed with osmium tetroxide also suggests the presence of unsaturated lipid or other reducing compounds. It is not known whether they are secretion or absorption granules, although Peachey and Rasmussen (34) refer to them as secretion granules.

The serosal cells are suggested by Leaf (21) as the site of active sodium transport. The morphological data herein presented can neither confirm nor deny this proposal. The serosal cells have a meager endowment of cytoplasm and unimpressive mitochondria but have many vesicles.

The question of the location of the transport processes is still open.

This investigation was supported in part by United States Public Health Service grants no. B-401 (C8) and no. 2G-136 (C4).

The author wishes to express his deepest gratitude to Dr. H. Stanley Bennett for suggesting this project, providing the opportunity for its study, and giving encouragement and advice during the early period of work. Thanks are also extended to Dr. John Luft for his guidance and patient help throughout the study and to Dr. N. B. Everett for his instruction in radioautography and his encouragement. He also wishes to thank Dr. R. L. Wood and his colleagues in the Department of Anatomy for their valuable suggestions and criticisms.

Received for publication, July 10, 1962.

BIBLIOGRAPHY

1. Bennett, H. S., The concepts of membrane flow and membrane vesiculation as mechanisms for active transport and ion pumping, *J. Biophysic. and Biochem. Cytol.*, 1956, **2,** No. 4, suppl., 99.
2. Bennett, H. S., and Luft, J. H., *s*-Collidine as a basis for buffering fixatives, *J. Biophysic. and Biochem. Cytol.*, 1959, **6,** 113.
3. Bennett, H. S., Luft, J. H., and Hampton, J. C., Morphological classifications of vertebrate blood capillaries, *Am. J. Physiol.*, 1959, **196,** 381.
4. Bentley, P. J., The effects of neurohypophysial extracts on water transfer across the wall of the isolated urinary bladder of the toad *Bufo marinus*, *J. Endocrinol.*, 1958, **17,** 201.
5. Bentley, P. J., The effects of vasopressin on the short circuit current across the wall of the isolated bladder of the toad, *Bufo marinus*, *J. Endocrinol.*, 1960, **21,** 161.
6. Biedermann, W., Electromotive action of epithelial and gland cells, *in* Electrophysiology, (F. A. Welby, translator), London, Macmillan and Co., Ltd., 1896, **1,** 461.
7. Burgos, M., The role of amorphous cellular coatings in active transport, *Anat. Rec.*, 1960, **137,** 171.
8. Choi, J. K., Electron microscopic study on the transitional epithelium of the toad bladder, *J. Appl. Physics*, 1960, **31,** 1632.
9. Choi, J. K., Light and electron microscopy of toad urinary bladder, *Anat. Rec.*, 1961, **139,** 214.
10. Choi, J. K., Electron microscopy of absorption of tracer materials by toad (*Bufo marinus*) bladder epithelium, *Anat. Rec.*, 1962, **142,** 222.

11. CRABBE, J., Stimulation of active sodium transport by the isolated toad bladder with aldosterone *in vitro*, *J. Clin. Inv.*, 1961, **40,** 2103.
12. DALTON, A. J., and ZEIGEL, R. F., A simplified method of staining thin sections of biological material with lead hydroxide for electron microscopy, *J. Biophysic. and Biochem. Cytol.*, 1960, **7,** 409.
13. DAVSON, H., and DANIELLI, J. F., The Permeability of Natural Membranes, (H. Davson and J. F. Danielli, editors), 2nd edition, Cambridge, University Press, 1952.
14. EVERETT, N. B., RIEKE, W. O., REINHARDT, W. O., and YOFFEY, J. M., Radioisotopes in the study of blood cell formation with special reference to lymphocytopoiesis, *in* Ciba Foundation Symposium on Haemopoiesis, London, J. and A. Churchill, Ltd., 1960, 43.
15. EWER, R. F., The effect of pituitrin on fluid distribution in *Bufo regularis Reuss*, *J. Exp. Biol.*, 1952, **29,** 173.
16. FARQUHAR, M. G., and PALADE, G. E., Tight intercellular junctions, *in* Abstracts, First Annual Meeting of the American Society for Cell Biology, Chicago, 1961, 57.
17. FRALEY, E. E., and WEISS, L., An electron microscopic study of the lymphatic vessels in the penile skin of the rat, *Am. J. Anat.*, 1961, **109,** 85.
18. ITO, S., The endoplasmic reticulum of gastric parietal cells, *J. Biophysic. and Biochem. Cytol.*, 1961, **11,** 333.
19. KOEFOED-JOHNSEN, V., and USSING, H. H., Ion transport, *in* Mineral Metabolism, (C. L. Comar and F. Bronner, editors), New York, Academic Press, Inc., 1960, **1,** Part A.
20. LAVDOWSKY, M., Die feinere Struktur und die Nervenendigungen, *Arch. Anat., Physiol. u. wissensch. Med.*, 1872, 55.
21. LEAF, A., Some actions of neurohypophyseal hormones on a living membrane, *J. Gen. Physiol.*, 1960, **43,** No. 5, suppl., 175.
22. LEAF, A., ANDERSON, J., and PAGE, L. B., Active sodium transport by the isolated toad bladder, *J. Gen. Physiol.*, 1958, **41,** 657.
23. LEAF, A., PAGE, L. B., and ANDERSON, J., Respiration and active sodium transport of isolated toad bladder, *J. Biol. Chem.*, 1959, **234,** 1625.
24. LILLIE, R. D., Histopathologic Technic and Practical Histochemistry, 2nd edition, New York, Blakiston Press, 1954.
25. LIST, J. H., Ueber einzellige Drüsen (Becherzellen) im Blasenepithele der Amphibien, *Arch. mikr. Anat.*, 1887, **29,** 147.
26. LUFT, J. H., Permanganate—a new fixative for electron microscopy, *J. Biophysic. and Biochem. Cytol.*, 1956, **2,** 799.
27. LUFT, J. H., Improvements in epoxy resin embedding methods, *J. Biophysic. and Biochem. Cytol.*, 1961, **9,** 409.
28. MILLONIG, G., A modified procedure for lead staining of thin sections, *J. Biophysic. and Biochem. Cytol.*, 1961, **11,** 736.
29. MOWRY, R. W., Improved procedure for the staining of acidic polysaccharides by Müller's colloidal (hydrous) ferric oxide and its combination with the Feulgen and the periodic acid–Schiff reactions, *Lab. Inv.*, 1958, **7,** 566.
30. MUIR, A. R., and PETERS, A., Quintuple-layered membrane junctions at terminal bars between endothelial cells, *J. Cell Biol.*, 1962, **12,** 443.
31. PAK POY, R. F. K., and BENTLEY, P. J., Fine structure of the epithelial cells of the toad urinary bladder, *Exp. Cell Research*, 1960, **20,** 235.
32. PALAY, S. L., The morphology of secretion, *in* Frontiers in Cytology, (S. L. Palay, editor), New Haven, Yale University Press, 1958, 305.
33. PALAY, S. L., and KARLIN, L. J., An electron microscopic study of the intestinal villus. II. The pathway of fat absorption, *J. Biophysic. and Biochem. Cytol.*, 1959, **5,** 373.
34. PEACHEY, L. D., and RASMUSSEN, H., Structure of the toad's urinary bladder as related to its physiology, *J. Biophysic. and Biochem. Cytol.*, 1961, **10,** 529.
35. PEASE, D. C., Fine structures of the kidney seen by electron microscopy, *J. Histochem. and Cytochem.*, 1955, **3,** 295.
36. REVEL, J. P., NAPOLITANO, L., and FAWCETT, D. W., Identification of glycogen in electron micrographs of thin tissue sections, *J. Biophysic. and Biochem. Cytol.*, 1960, **8,** 575.
37. RHODIN, J., Correlation of ultrastructural organization and function in normal and experimentally changed proximal convoluted tubule cells of the mouse kidney, Stockholm, Karolinska Institute, Aktiebolaget Godvil, 1954.
38. RHODIN, J., and DALHAM, T., Electron microscopy of the tracheal ciliated mucosa in rat, *Z. Zellforsch.*, 1956, **44,** 345.
39. ROBERTSON, J. D., New observations on the ultrastructure of the membranes of frog peripheral nerve fibers, *J. Biophysic. and Biochem. Cytol.*, 1957, **3,** 1043.
40. ROBERTSON, J. D., Structural alterations in nerve fibers produced by hypotonic and hypertonic solutions, *J. Biophysic. and Biochem. Cytol.*, 1958, **4,** 349.
41. SCHIEFFERDECKER, P., Zur Kenntniss des Baues der Schleimdrüsen, *Arch. mikr. Anat.*, 1884, **23,** 382.
42. SEDAR, A. W., Electron microscopy of the oxyntic cell in the gastric glands of the bullfrog (*Rana*

catesbiana). I. The non-acid-secreting gastric mucosa, *J. Biophysic. and Biochem. Cytol.*, 1961, **9**, 1.

43. SEDAR, A. W., Electron microscopy of the oxyntic cell in the gastric glands of the bullfrog, *Rana catesbiana*. II. The acid-secreting gastric mucosa, *J. Biophysic. and Biochem. Cytol.*, 1961, **10**, 47.
44. SOTELO, J. R., and PORTER, K. R., An electron microscope study of the rat ovum, *J. Biophysic. and Biochem. Cytol.*, 1959, **5**, 327.
45. STEEN, W. B., On the permeability of the frog's bladder to water, *Anat. Rec.*, 1929, **43**, 215.
46. WATSON, M. L., Staining of tissue sections for electron microscopy with heavy metals, *J. Biophysic. and Biochem. Cytol.*, 1958, **4**, 475.
47. WOOD, R. L., and HOWARD, C. C., Use of fine grain positive sheet film for electron microscopy, *J. Biophysic. and Biochem. Cytol.*, 1959, **5**, 181.
48. YAMADA, E., The fine structure of the gall bladder epithelium of the mouse, *J. Biophysic. and Biochem. Cytol.*, 1955, **1**, 445.